1-1-2004

Investigation of Order Parameters and Critical Coupling for the Peierls Extended Hubbard Model at One-Quarter Filling

Rahul Padmakar Hardikar

INVESTIGATION OF ORDER PARAMETERS AND CRITICAL COUPLING FOR THE PEIERLS EXTENDED HUBBARD MODEL AT ONE-QUARTER FILLING

By

Rahul Padmakar Hardikar

A Thesis
Submitted to the Faculty of
Mississippi State University
in Partial Fulfillment of the Requirements
for the Degree of Master of Science
in Physics
in the Department of Physics and Astronomy

Mississippi State, Mississippi

December 2004

INVESTIGATION OF ORDER PARAMETERS AND CRITICAL

COUPLING FOR THE PEIERLS EXTENDED HUBBARD

MODEL AT ONE-QUARTER FILLING

By

Rahul Padmakar Hardikar

Approved:

Rudolf Torsten Clay Assistant Professor of Physics and Astronomy. (Major Professor)	Mark A. Novotny Professor of Physics and Astronomy, and Department Head (Committee Member)
Jeff A. Winger Professor of Physics and Astronomy (Committee Member)	David L. Monts Professor of Physics and Astronomy, and Graduate Coordinator, Department of Physics and Astronomy

Phil Oldham
Dean of the College of Arts and Sciences

Name: Rahul Padmakar Hardikar

Date of Degree: December 11, 2004

Institution: Mississippi State University

Major Field: Physics

Major Professor: Dr. Rudolf Torsten Clay

Title of Study: INVESTIGATION OF ORDER PARAMETERS AND CRITICAL COUPLING FOR THE PEIERLS EXTENDED HUBBARD MODEL AT ONE-QUARTER FILLING

Pages in Study: 52

Candidate for Degree of Master of Science

The determination of the phase boundary between the charge density wave and the Luttinger Liquid phase for the one-dimensional Peierls extended Hubbard model is done using Stochastic Series Expansion and comparison is done with the phase boundary for the Extended Hubbard model. The result of adding an electron-phonon interaction is that the charge density wave phase weakens.

The energy autocorrelation time is reported for the Extended Hubbard Model and the Peierls Hubbard Model. For coupling near and above the critical coupling the autocorrelation time increases exponentially.

Also investigated is the presence of a spin gap and the critical value of phonon coupling with respect to two parameters, (1) the bare phonon frequency and (2) different U, at one-quarter filling.

DEDICATION

To my wife Poonam and my elders.

ACKNOWLEDGMENTS

My sincere gratitude to my major advisor, Dr. Rudolf Torsten Clay, for his magnanimity in expending time and effort to guide me through my graduate studies and also for his critical and resourceful suggestions and advice in the thesis process and letting me use his Stochastic Series Expansion code as a tool to do my thesis work. I also express my appreciation to the committee members, Dr. Mark A. Novotny, Dr. Jeff A. Winger and Dr. David L. Monts, for their invaluable advice and encouragement. Thanks to all personnel at the Engineering Research Center (ERC), Center for Computational Sciences (CCS) as well as professors and staff of the Department of Physics and Astronomy at the Mississippi State University.

TABLE OF CONTENTS

CHAPTER Page

LIST OF TABLES

LIST OF FIGURES

LIST OF SYMBOLS, ABBREVIATIONS, AND NOMENCLATURE

H Hamiltonian

EHM Extended Hubbard Model

PEH Peierls Extended Hubbard Model

t hopping interaction (bond strength)

U onsite interaction

V intersite interaction

μ chemical potential

α phonon coupling

ω bare phonon frequency

$c^{\dagger}_{i,\sigma}$ creation operator

$c_{i,\sigma}$ anhillation operator

α_c critical phonon coupling

CDW charge density wave

SDW spin density wave

BOW bond order wave

χ_c charge susceptibility

χ_b bond order susceptibility

χ_s spin susceptibility

S_c Charge structure factor

S_s Spin structure factor

CHAPTER I

INTRODUCTION

1.1 Introduction

The Hubbard model is "a highly over-simplified model" of strongly interacting electrons in a solid [1]. This model includes quantum mechanical motions of electrons and also the repulsive Coulomb interaction between electrons. It exhibits phenomenon such as a metal-insulator transition, anti-ferromagnetism, ferrimagnestism and Tomonaga-Luttinger liquid behaviour. In this thesis we will be concentrating on the effect of the electron-phonon (e-ph) interaction in the Hubbard model.

We first summarize the Hubbard model and its parameters. Let lattice L be a collection of sites $1, 2, ...N$ where each lattice site corresponds to an atomic site or a molecular orbital in a crystal. Each site has one electron orbital that is non-degenerate in the case of the standard model. The electrons in other orbitals do not play a significant role in the low-energy physics and hence can be neglected [28].

The Hubbard Hamiltonian is given as follows:

$$H = \sum_{i,j \in L}^{N} \sum_{\sigma=\uparrow,\downarrow} t_{ij} \left({c^{\dagger}}_{i,\sigma} c_{j,\sigma} + h.c \right) + \sum_{i \in L}^{N} U_i n_{i,\uparrow} n_{i,\downarrow} \tag{1.1}$$

where $h.c$ indicates the Hermitian conjugate and $n_{i\sigma} = c^{\dagger}_{i\sigma} c_{i\sigma}$ is the number operator.

The one dimensional variant of the Hubbard model is given by:

$$H = -t \sum_{i=1,\sigma=\uparrow\downarrow}^{N} \left({c^{\dagger}}_{i\sigma} c_{i+1\sigma} + h.c \right) + U \sum_{i=1}^{N} n_{i\uparrow} n_{i\downarrow} \tag{1.2}$$

This Hamiltonian incorporates on-site interactions U and the hopping term involving t. In this thesis we will be dealing with the Extended Hubbard model which has a term which includes inter-site interactions in addition to the two described above. This term helps to model the effect of long-ranged Coulomb interactions. We also focus on one dimensional lattices. The Extended Hubbard model (EHM) Hamiltonian in 1D is:

$$H_{EHM} = -t \sum_{i=1,\sigma=\uparrow\downarrow}^{N} \left({c^{\dagger}}_{i\sigma} c_{i+1\sigma} + h.c \right) + U \sum_{i=1}^{N} n_{i\uparrow} n_{i\downarrow} + V \sum_{i=1}^{N} n_i n_{i+1} \tag{1.3}$$

where $n_{i\sigma} = {c^{\dagger}}_{i\sigma} c_{i+1\sigma}$, $n_i = n_{i\uparrow} + n_{i\downarrow}$ and ${c^{\dagger}}_{i\sigma}$ $(c_{i\sigma})$ denotes an operator which creates (annihilates) an electron with spin $\sigma = \uparrow$ or $\downarrow$ at site $i \in L$.

In addition to these parameters there is one implicit parameter known as "band filling". It is defined as $\rho = N_e/N$, where N_e is the total number of electrons ($\uparrow$ and $\downarrow$) and N is the number of sites. The value of ρ is determined by the material used e.g. for conducting polymers such as polyacetylene in their insulating state we have $\rho = 1$, or in other words they are "half filled". The "Bechgaard salts" have $\rho = 3/4$ if we consider the density of electrons and $\rho = 1/4$ i.e.; "quarter filled" if we consider holes. We will be studying various properties of substances at quarter filling in this thesis as it is the appropriate filling for a large class of organic superconductors.

The EHM is interesting because its one-dimensional (1D) version is appropriate for modeling conducting polymers, certain charge-transfer solids, and related materials [19].

The EHM has been studied extensively by various methods. It is believed to be "non-integrable", and does not have an exact solution except at $V = 0$ or $V \to \infty$ [24]. A good analytic insight in the weak coupling regime (small U and V) is provided by classic "g-ology" investigations [23, 10, 26] and more recent renormalization group [11] and bosonization studies. Methods like exact diagonalization calculations [7, 12] and Quantum Monte Carlo simulations [16, 17, 18, 21, 2] have resolved many questions at intermediate and strong coupling [9, 13, 8].

1.2 Phase Diagram

In this section we revisit the phase diagram of EHM and one by one discuss each of the phases in it.

1.2.1 Phase Diagram description

Throughout this thesis I will be referring to parameters such as U/t as U and so on unless specified. Fig:1.1 shows the phase diagram of the EHM for $U > 0$ and $V > 0$ at 1/4 filling. Except for very large V for which the system is Phase Separated (PS), there are two phases namely the ..1010.. Charge Density Wave (CDW) phase and the Luttinger Liquid phase. The ..1010.. CDW is a $4k_F$ charge modulation, while the Luttinger Liquid phase has uniform charge density. Fig:1.1 shows the critical values of V for the boundary between these two phases at 1/4 filling. As described in [4] in the limit $U \to \infty$ the critical

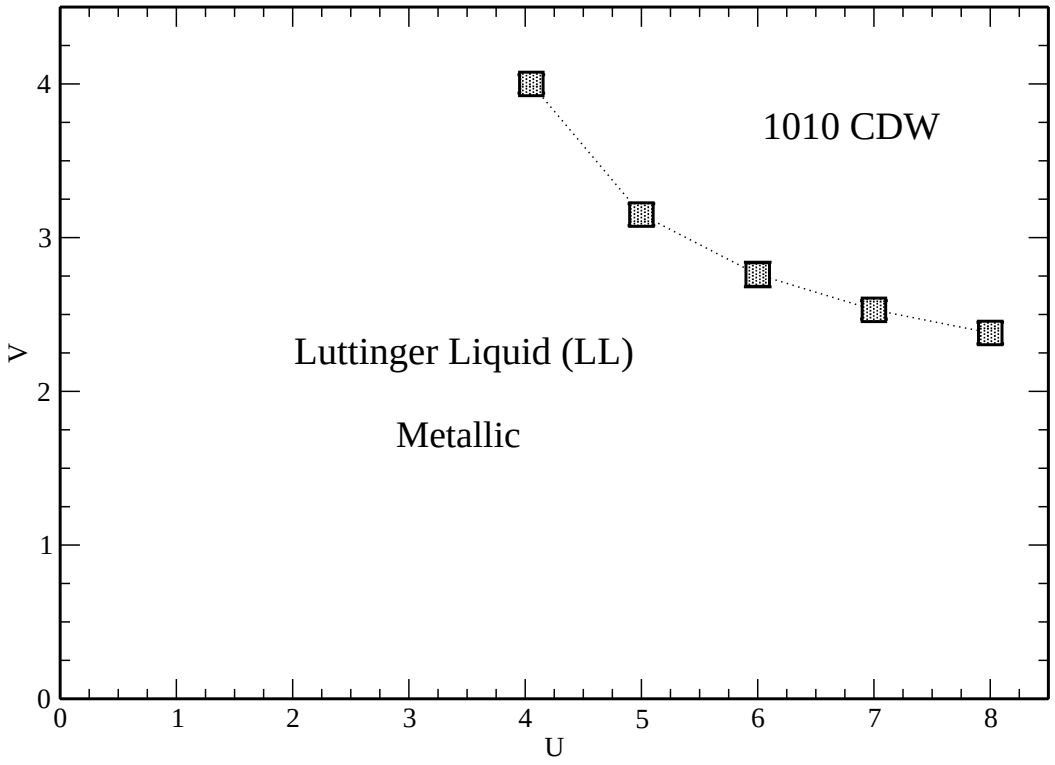

Figure 1.1 Phase Diagram for EHM at 1/4 filling.

value of V for the transition is $V_c = 2$. For $V \to \infty$ the phase boundary is at $U_c = 4$. For $U > U_c$ the system is in the $4k_F$ CDW phase while for $U < U_c$ the system is a LL.

In Chapter III we will observe the effects of adding e-ph interactions to EHM and see how it affects the phase boundary.

1.2.2 The ..1010.. Charge Density Wave (CDW)

This type of charge ordering is observed in quasi 1D charge transfer solid (CTS) systems. It is a Wigner crystal-like state. The site occupancy "1" corresponds to $0.5 + \epsilon$ and "0" corresponds to $0.5 - \epsilon$, with ϵ being an important measurable quantity. The ..1010.. corresponds to a $4k_F$ CDW with a spatial period 2, where $k_F = \pi/2a$, in the absence of Coulomb interaction is called the Fermi wave vector, a is the lattice constant. The ..1010.. state requires both U (on-site Coulomb repulsion) and V (inter-site Coulomb repulsion) to be greater than some critical value $V_c\,(U)$ [4].

1.2.3 Luttinger Liquid (LL)

The Luttinger Liquid is based on the properties of Tomonaga-Luttinger model [29, 22]. It is useful in describing one-dimensional models of interacting particles which have properties differing sharply from the properties of conventional Fermi liquids [14, 15]. The following are characteristics of a Luttinger liquid: (i) vanishing of the quasi-particle residue at the Fermi surface, showing continuity at the Fermi surface and the power-law behaviour replacing it, (ii) existence of gap-less, collective excitations modes. (iii) charge

and spin properties separate and all correlation functions of the model can be expressed by a single exponent K.

It has been established that the one dimensional Hubbard model is a two component Luttinger liquid (K_ρ, K_σ) in much of its phase diagram. Luttinger Liquid theory provides hyper-scaling relations among exponents of charge-charge, spin-spin and single-particle correlation functions. The following are the relations established for Luttinger liquids:

$$E(N) = E_\infty - \frac{1}{N^2}\frac{\pi c}{6}(v_c + v_s) \tag{1.4}$$

$$K_\rho = \frac{\pi}{2}\rho^2 \kappa v_c \tag{1.5}$$

$$D_c = \frac{1}{\pi} K_\rho v_c \tag{1.6}$$

where N is the system size, κ is the compressibility, c is central charge, D_c is the Drude weight, and v_c is the charge velocity. Eqn.1.5 and Eqn.1.6 for a given v_c and κ, provide two different ways to calculate K_ρ. $K_\rho < 1$ indicates charge repulsive interaction, while $K_\rho > 1$ indicates charge attractive (Superconducting (SC)) interactions. The system can be considered a Luttinger Liquid if the above relations are consistent. We can determine the system phase boundaries by plotting contours of K_ρ, as K_ρ determines which fluctuations are dominant for a Luttinger Liquid [20].

1.2.4 Spin-Peierls (SP) state

SP transitions occur in 1D by coupling of the electron spin to the phonon modes. The resulting ground state is non-magnetic (spin gapped). The SP transition is predicted

to occur for weak spin-lattice coupling in the limit of adiabatic phonons and in the anti-adiabatic limit the transition can occur only above a critical value of the coupling. When we add the effects of e-ph interaction to the extended Hubbard model, the resulting model is called a "Peierls-Extended Hubbard" (PEH) model.

The phonon Hamiltonian is given as follows:

$$\begin{aligned} H = -t \sum_{i=1,\sigma}^{N} \left(1 + \alpha[a_i^\dagger + a_i]\right) \left(c_{i+1,\sigma}^\dagger c_{i,\sigma} + c_{i,\sigma}^\dagger c_{i+1,\sigma}\right) \\ +\mu \sum_i n_i + U \sum_i \left(n_{i,\uparrow} - \tfrac{1}{2}\right) \left(n_{i,\downarrow} - \tfrac{1}{2}\right) \\ +V \sum_i (n_i - 1)(n_{i+1} - 1) + \omega_0 \sum_i a_i^\dagger a_i \end{aligned} \tag{1.7}$$

There are two kinds of phonons (a) bond phonons and (b) site phonons. We will consider only bond phonons here.

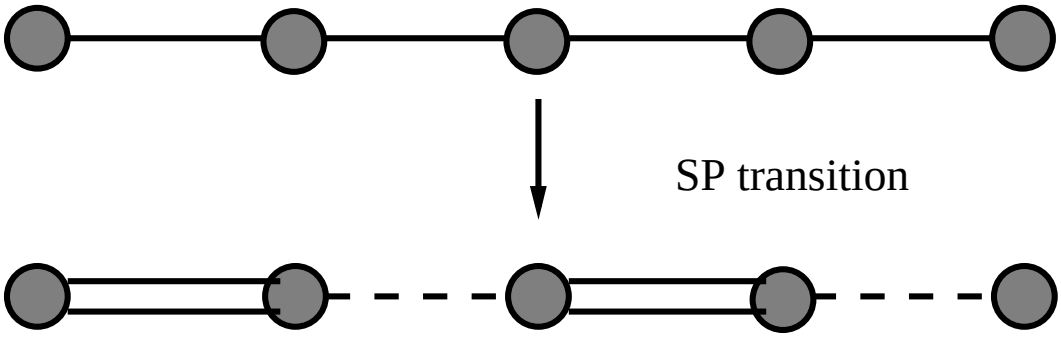

Figure 1.2 SP transition for 1/2 filled case. At this transition the lattice dimerizes.

The SP transition is different for half-filling and quarter filling. The half filling case is very well studied. In this case the transition corresponds to a dimerization of the lattice as shown in fig:1.2. The SP transition in the quarter filled case can occur in two ways: either

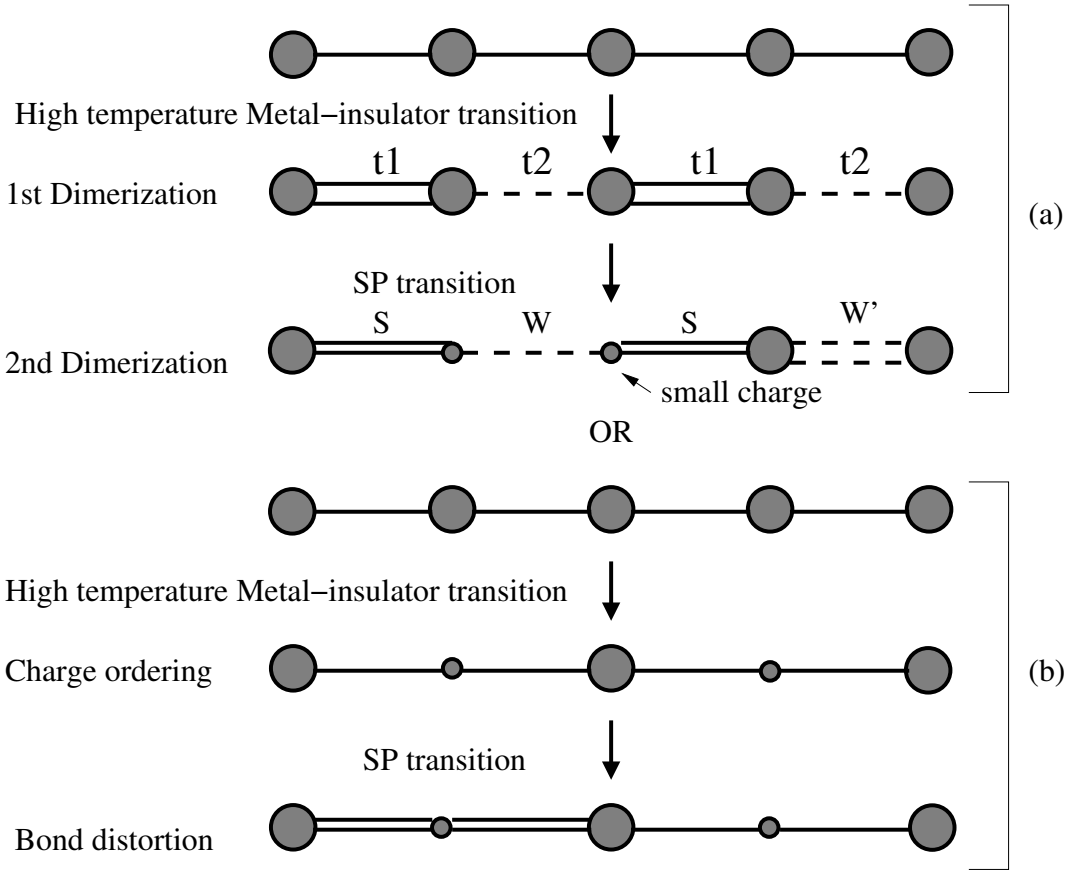

Figure 1.3 SP transtion for 1/4 filled case.

(1) by second dimerization as shown in fig:1.3.a , or (2) after the ..1010.. Charge ordering (CO) as shown int fig:1.3.b. Different bond distortions are expected in these two different situations.

1.2.5 Goals of this Thesis

- Try to characterize numerical methods to study the 1D PEH.
- We intend to map out the phase diagram at quarter filling for the PEH.
- Investigate details of SP transitions at quarter filling.
- Compare our results for quarter filling with the previous work done for half filling.

CHAPTER II

OVERVIEW OF METHODS

2.1 Stochastic Series Expansion (SSE)

The Stochastic Series Expansion method is one of the advances in quantum Monte Carlo (QMC) algorithms which have opened up several classes of quantum many-body models to large-scale numerical studies which were only possible for classical studies before. The SSE, an extension of Handscomb's method, is a power series expansion of the partition function. This method incorporates (i) the elimination of the systematic error of the Trotter decomposition and (ii) the development of loop-cluster algorithms for efficient sampling in the quantum mechanical configuration space. This method also offers dramatic speed-ups, in many cases a reduction in autocorrelation time (discussed in the next section) by many orders of magnitude. This feature allows the study of system sizes much larger than what were possible before with local sampling algorithms. One important property of loop-cluster algorithms (world-line, SSE operator loop and world-line worms) is that they are efficient also in the presence of external fields. The SSE method with operator loop-update is a very powerful method for quantum spin systems (including magnetic field), boson systems (including chemical potential), and 1-D Fermionic systems.

2.1.1 Overview of SSE

As mentioned above this method is a power series expansion of the partition function given:

$$Z = Tr\{e^{\beta H}\} = \sum_{\alpha} \sum_{n=0}^{\infty} \frac{(-\beta)^n}{n!} \langle \alpha | H^n | \alpha \rangle \tag{2.1}$$

Here the trace is expressed in terms of a sum over diagonal matrix elements of the basis $|\alpha\rangle$. The SSE method gives a discrete nature to configuration space, which can be sampled without floating point operations. This is an advantage over continuous-time world-line methods. Eqn:2.1 can also be expressed as

$$Z = \sum_{\alpha} \sum_{n=0}^{\infty} \sum S_n (-1)^{n_2} \frac{\beta^n}{n!} \langle \alpha | \Pi_{i=1}^{n} H_{a_i b_i} | \alpha \rangle \tag{2.2}$$

where β is inverse temperature, n_2 is the total number of off-diagonal spin-flipping operators in S_n ($S_n = [a_1, b_1], [a_2, b_2], ...[a_n, b_n]$), a_i belongs to 1=diagonal, 2=off-diagonal and b_i belongs to 1...N_b is the bond index operator.

In Eqn:2.2

$$|\alpha(p)\rangle \sim \Pi_{i=1}^{p} H_{a_i b_i} |\alpha\rangle \tag{2.3}$$

represents normalized states. All the basis states are either the same or they differ by a flipped pair of spins. The term has to be periodic in imaginary time i.e. $|\alpha(n)\rangle = |\alpha(0)\rangle$, to contribute to the partition function. For the expansion to be positive definite on a bipartite lattice n_2 should be even. This way the configurations can be sampled using MC techniques without a sign problems.

The partition function can be simplified by removing the sum over n by truncating the expansion at the maximum power $n = M$ and inserting $M - n$ unit operators in the operator products in all possible ways. This is given as:

$$Z = \sum_{\alpha} \sum_{S_M} \beta^n \frac{(M-n)!}{M!} \langle \alpha | \Pi_{i=1}^{M} H_{a_i b_i} | \alpha \rangle \tag{2.4}$$

where n will be the number of non-null operators.

The SSE method follows two updating schemes (1) Diagonal Update and (2) Loop Update. The diagonal update involves a single diagonal operator, which changes the expansion order n by ± 1. It is applicable to terms like U, V and μ in the EHM which are diagonal terms in the Hamiltonian. The loop update is applicable to off-diagonal or the terms involving hopping in the EHM Hamiltonian. This loop update accomplishes substitutions for different number of states thereby resulting in spin flipping in several propagated states. The expansion order n does not change and hence its convenient to work with the original sequence S_n instead of S_M or the reduced sequence. Detailed description of the SSE method can be found in [27].

2.2 Checking Methods

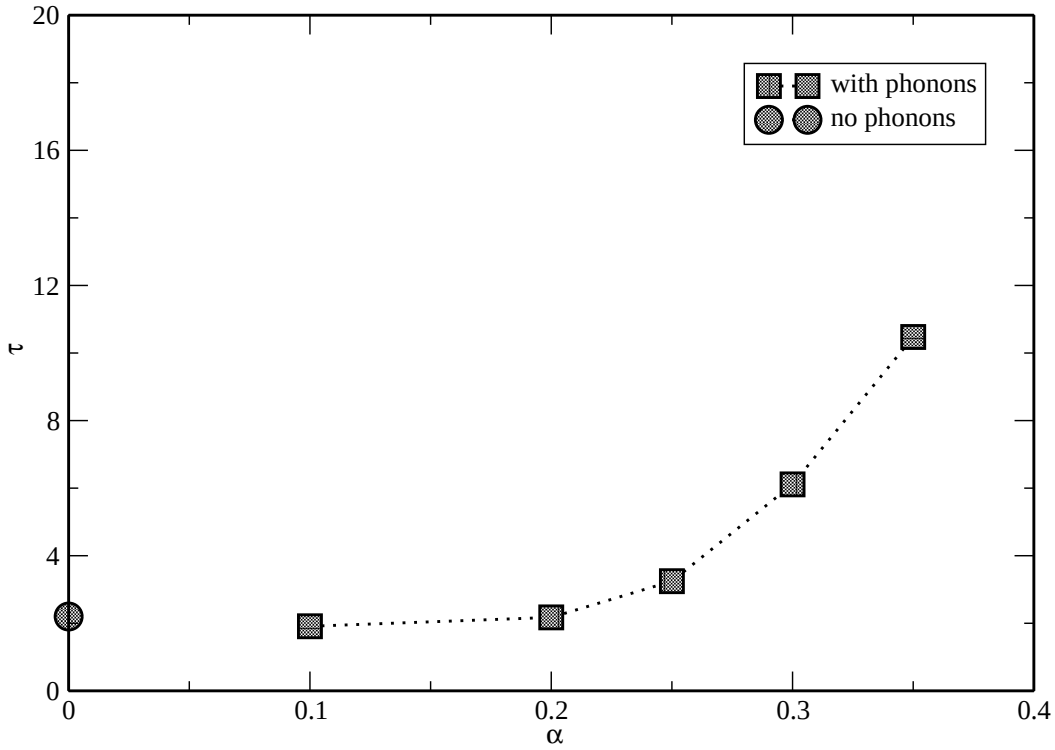

Figure 2.1 Comparison of Energy autocorrelation time between EHM (filled circle) and PEH (filled squares) as a function of e-ph coupling α.

2.2.1 Autocorrelation time τ

The integrated autocorrelation time for an observable O is given as:

$$\tau_{int}[O] = \frac{1}{2} + \sum_{t=1}^{\infty} A_O(t) \tag{2.5}$$

where $A_O(t)$ is the autocorrelation function. This function gives a quantitative measure of the efficiency of a Monte Carlo sampling scheme in generating statistically independent configurations. It is given by:

$$A_O(t) = \langle O(i+t)O(i)\rangle - \langle O(i)\rangle^2 \Big\langle \Big\langle O(i)^2 \Big\rangle - \langle O(i)\rangle^2 \Big\rangle \tag{2.6}$$

where i and t are Monte Carlo times. The $\langle ...\rangle$ indicates the average over time i. This function decays exponentially as $\sim e^{\frac{-t}{\tau(O)}}$, where $\tau(O)$ is the slowest mode of the simulation to which the observable O couples. The autocorrelation time is the autocorrelation measure for the maximum practical utility.

Fig:2.1 shows the comparison of the energy autocorrelation time (τ) for the EHM ($\alpha = 0$ and $\omega = 0$) and the PEH ($\alpha = 0.1$ and $\omega = 0.2$) for $L = 32$ and $\beta = 32$ with $U = 6$ and $V = 1$. For $\alpha \langle \alpha_c$ the autocorrelation time is comparable to that of the EHM where $\alpha = 0$, but as α approaches α_c, τ increases exponentially. Hence for $\alpha > \alpha_c$ it is hard to get reliable data because of the long autocorrelation time of the calculations. This is the reason that we were unable to determine the magnitude of the spin gap for quarter filled system. Just above α_c the spin gap is very small and it is hard numerically to compute the magnitude of the spin gap. Also the spin gap is zero at $\alpha = \alpha_c$.

2.3 Lanczos Method

The Lanczos method is one of the exact diagonalization methods which can determine a few of the lowest eigenvalues and eigenvectors of a matrix. In this method a basis is constructed in which the Hamiltonian, here the EHM, has a tridiagonal representation.

Following is a brief idea about the steps involved in Lanczos method.

To get a ground-state using this method we first choose an arbitrary vector $|\phi_0\rangle$ in Hilbert space, satisfying the condition that there should be a non-zero overlap between the actual ground state, say $|\psi_0\rangle$ and the initial state $|\phi_0\rangle$. If $|\psi_0\rangle$ is unknown then an initial state with randomly chosen coefficients in the working basis is used. A new vector can be found by operating the Hamiltonian $\hat{H}$ on the initial vector and subtracting the projection of a new vector on $|\phi_0\rangle$ given as:

$$|\phi_1\rangle = \hat{H}|\phi_0\rangle - \frac{\langle\phi_0|\hat{H}|\phi_0\rangle}{\langle\phi_0|\phi_0\rangle}|\phi_0\rangle \tag{2.7}$$

satisfying $\langle\phi_0|\phi_1\rangle = 0$. We get a orthogonal basis by recursively doing the above procedure. Following is the general form for the above Eqn:2.7

$$|\phi_{n+1}\rangle = \hat{H}|\phi_n\rangle - a_n|\phi_n\rangle - b_n^2|\phi_{n-1}\rangle \tag{2.8}$$

where $n = 0, 1, 2, \cdots$ and

$$a_n = \frac{\langle\phi_n|\hat{H}|\phi_n\rangle}{\langle\phi_n|\phi_n\rangle}, \;\; b_n^2 = \frac{\langle\phi_n|\phi_n\rangle}{\langle\phi_{n-1}|\phi_{n-1}\rangle} \tag{2.9}$$

and $b_0|\phi_{-1}\rangle = 0$.

The Hamiltonian matrix becomes

$$\begin{pmatrix} a_0 & b_1 & 0 & 0 & . & . \\ b_1 & a_1 & b_2 & 0 & . & . \\ 0 & b_2 & a_2 & b_3 & . & . \\ 0 & 0 & b_3 & a_3 & . & . \\ . & . & . & . & & \\ . & . & . & . & & \end{pmatrix}$$

Hence we get a tridiagonal matrix. After obtaining such a matrix it can be diagonalized using standard LAPACK library subroutines [6].

This method is limited in the sense that it can be applied to small system sizes (16 sites at quarter filling) due to the exponential growth of the size of H with N. We use this method to verify the results of the SSE method in this thesis. A C code for the Lanczos method is given in the Appendix A.

CHAPTER III

RESULTS

3.1 Calculation of Phase Boundary between ..1010.. CDW and LL

Does the addition of phonons change the ..1010.. - LL boundary at quarter filling? In this section we describe some methods to determine the phase boundary of the PEH and compare the results with the phase boundary of the EHM.

In this section we attempt to find the phase boundary between the metallic (LL) phase and the insulator (..1010.. CDW) phase for the PEH at quarter filling. The the LL phase has no charge ordering. The presence of LL phase can be determined by investigating some basic properties of LL such as K_ρ.

There are two different methods to determine the phase boundary. The first method uses the standard technique of finite-size scaling of the $q = 4k_F$ charge susceptibility given by:

$$\chi_\rho(q) = \frac{1}{N}\sum_{j,l} e^{iq(j-l)} \int_0^\beta d\tau \langle n_j(\tau) n_l(0)\rangle \tag{3.1}$$

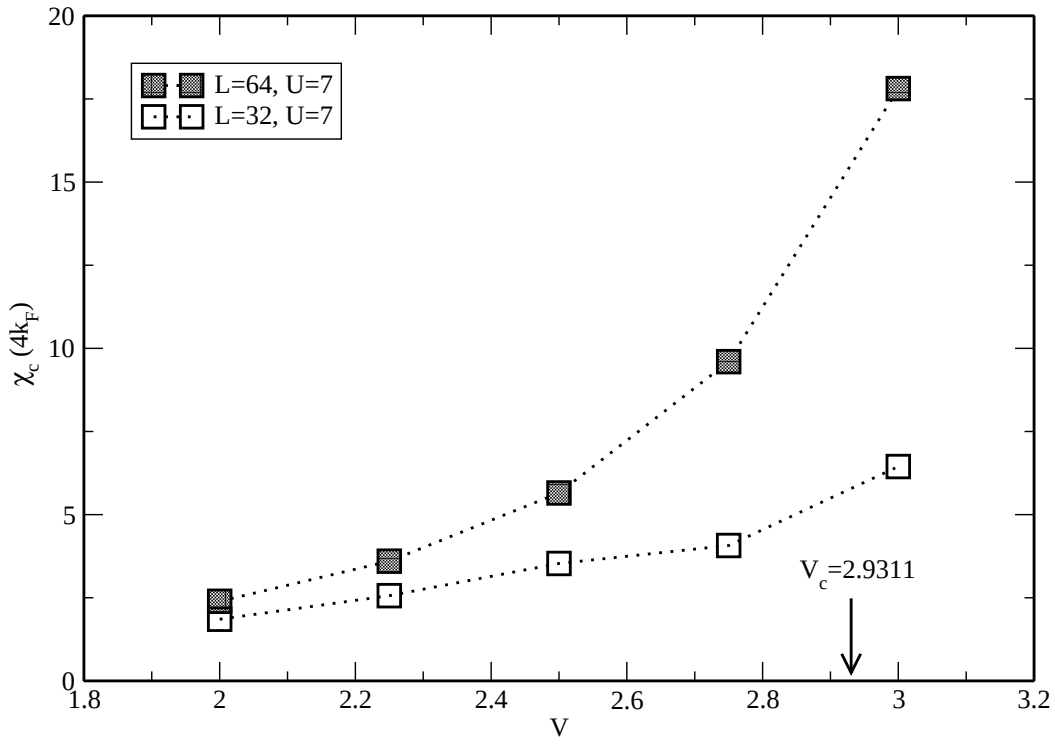

Figure 3.1 Determination of V_c using charge susceptibility $4k_F$ data for $U = 7$ for $L = 32$ and $L = 64$, $\alpha = 0.1$ and $\omega = 0.25$. There is an increase in the value of $\chi_c(4k_F)$ near V_c, and χ_c at $4k_F$ diverges with system size in the ..1010.. phase.

where N is the number of lattice sites, β is the inverse temperature, and $n_j(\tau)$ is the charge at site j at a imaginary time τ. This method make use of the fact that for the system to be in the ..1010.. CDW phase,

$$\chi_\rho(4k_F, N_1) - \chi_\rho(4k_F, N_2) > \chi_\rho(4k_F, N_2) - \chi_\rho(4k_F, N_3)$$

, where $N_1 > N_2 > N_3$ and N is the system size [3].

Fig:3.1 shows data points for the charge susceptibility $4k_F$ peaks for $U = 7$, $\omega = 0.25, \alpha = 0.1$ at quarter filling for system sizes L=32 and 64. We show the value of V_c which is calculated in Fig:3.2. In the above plot we cannot see a sharp increase in the charge susceptibility at a certain value of V. This can be seen only if we go to system sizes of the order L=128, where a sharp increase is seen at V_c.

The second method is much easier as compared to the first one, because it makes use of the static charge structure factor which can be more easily computed using SSE as compared to the charge susceptibility.

The later method makes the use of the fact that in the regime $V < V_c$ the system is a LL, with correlation functions governed by K_ρ. The value of V_c for ..1010.. phase is determined where $K_\rho \to 1/3$. The value of K_ρ is calculated from the $q \to 0$ limit of the static charge structure factor [3]. K_ρ is given by the slope of the charge structure factor in the long wavelength limit,

$$K_\rho = 1/\pi q S_q(q \to 0).$$

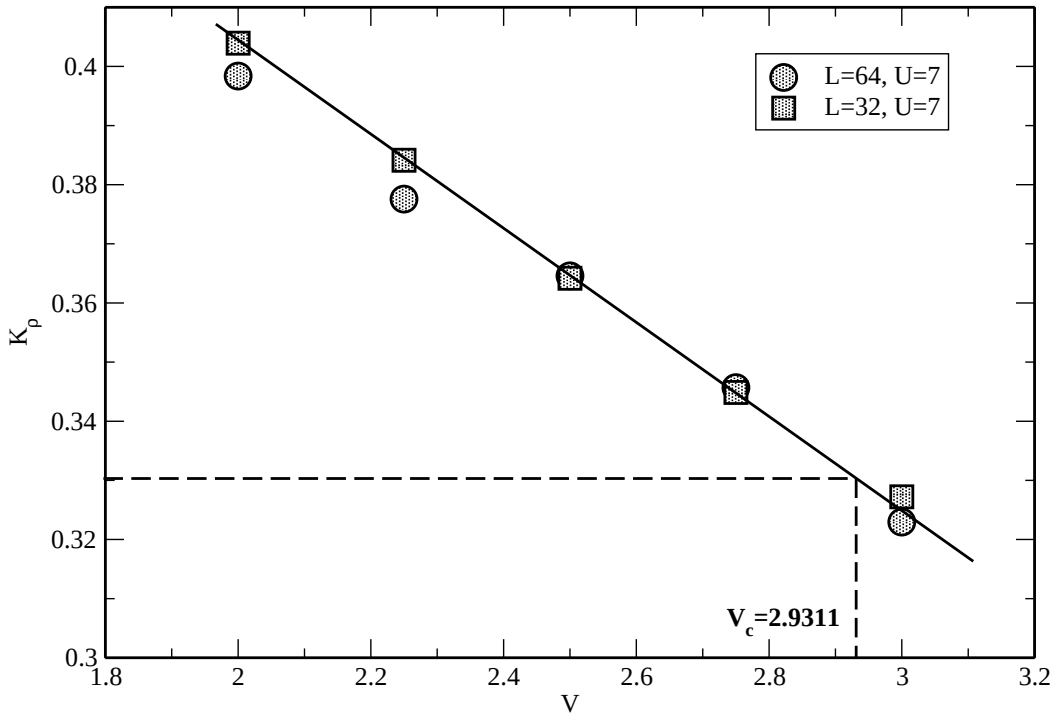

Figure 3.2 Determination of V_c using charge structure factor data for $U = 7$ for $L = 32$ and $L = 64$, $\alpha = 0.1$ and $\omega = 0.25$.

Fig:3.2 shows data points for the slope (K_ρ) of $S_q(q \to 0)$. Also shown is comparison for system sizes $L = 64$ (filled circles) and L=32 (filled squares). We fit a straight line for $L = 32$ and get the value for $V_c = 2.9311$.

Similarly we calculate the V_c for different U and get the phase boundary between the Luttinger Liquid phase and the ..1010.. CDW phase for the PEH as shown in next section.

3.2 Comparison of Phase Diagram of 1D EHM with the PEH

Following the second method described in the previous section we find the phase boundary between the ..1010.. CDW and the LL phase for quarter filling.

Fig:3.3 shows the comparison of phase boundary in case of 1D EHM and the PEH at quarter-filling. We observe that for finite $U > 0$, $V_c(U) \approx 2.5$ which is higher than the V_c for pure the EHM as mentioned in Introduction. Also for high $V > 0$ value of $U_c \sim 4$ which agrees with the pure EHM. It seems that at finite U the values for V_c get higher in case of the PEH than in case of the EHM.

This indicates that the presence of the bond phonon weakens the ..1010.. CDW phase.

3.3 How to calculate the spin gap?

In this section we describe some methods to determine the presence of a spin gap for a dimerized model at quarter filling. We also find the phase boundary between the Peierls and the dimerized insulator state. Also we compare our results with the half-filled case done in [25].

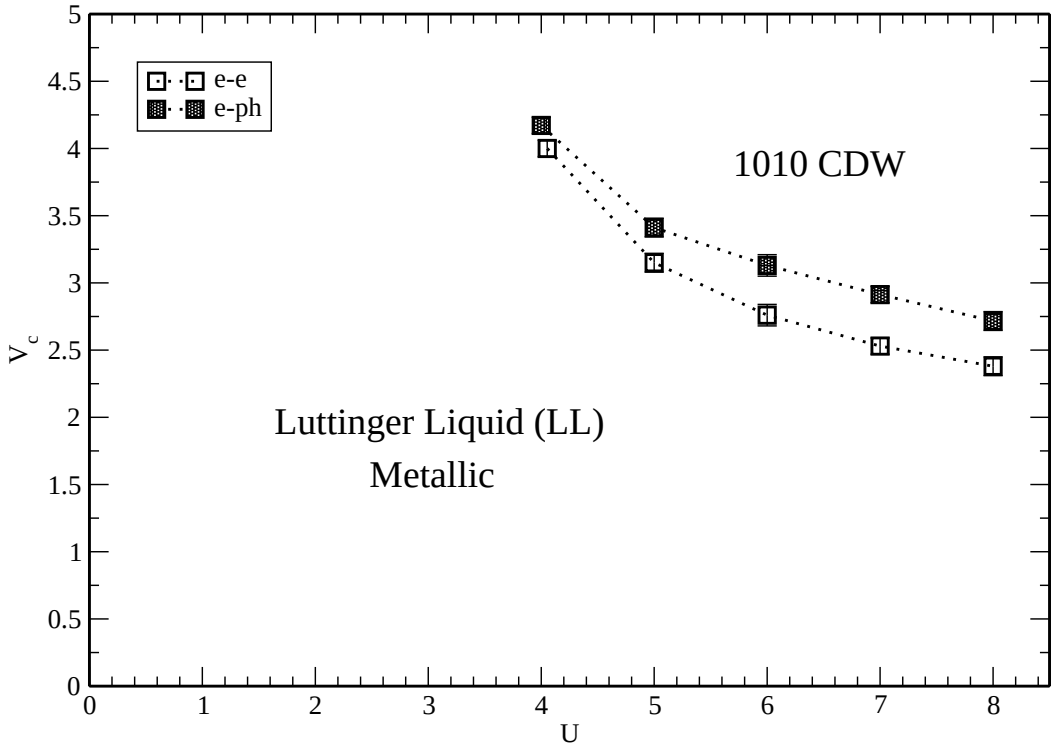

Figure 3.3 Phase Boundary comparison for EHM and PEH at quarter filling. For PEH parameters are L=64, $\alpha = 0.1$ and $\omega = 0.25$. Open squares-EHM data points, filled squares-PEH data points.

3.3.1 Spin Gap

So what exactly does a spin gap mean? A spin gap can be considered as a non-magnetic state in which a finite amount of energy is needed to flip spins at a particular site. So how can we detect the presence of a spin gap? To find out whether a system is spin gaped one can check that the spin susceptibility $\chi_\sigma(q) \to 0$ as $q \to 0$. A spin gap can also be shown if the spin structure factor $S_\sigma(q)$ approaches zero faster than linearly and when it falls below the line with slope π. The slope π corresponds to $K_\sigma = 1$ which means that there is no spin gap [5].

There are several ways to determine the presence of spin gap. As described in [25] the presence of Peierls phase can be shown if the $\chi_S(\pi)/N$ converges to 0. If $\chi_S(\pi)/N$ diverges logarithmically then it indicates the presence of a Mott insulator phase which in our case (1/4 filling and dimerized) corresponds to a Dimerized Insulator (DI) phase. This type of determination of a spin gap is not efficient if the spin gap is negligibly small. The other way to determine a spin gap efficiently is to study the behaviour of the spin structure factor given by Eqn:3.1.

In this thesis we study the behavior of the spin structure factor as $q \to 0$. This method is adopted because it efficiently detects even a very small spin gap. The way to do this is to observe behaviour of exponent K_σ given by the slope of the spin structure factor for $q \to 0$.

$$K_\sigma = \frac{1}{\pi}\mathrm{slope_{q\to 0}S_s(q)}.$$

If $K_\sigma \geq 1$ the system is not spin gapped, while if $K_\sigma < 1$ then it indicates the presence of a spin gap. The way in which the spin gap is known is that if $S_s(q)/q \to 1/\pi$ as $q \to 0$ then the ground state does not have a spin gap, but if $S_s(q)/q \to 0$ then it indicates a spin gap for the corresponding value of coupling. This is how the critical value of coupling α_c is obtained.

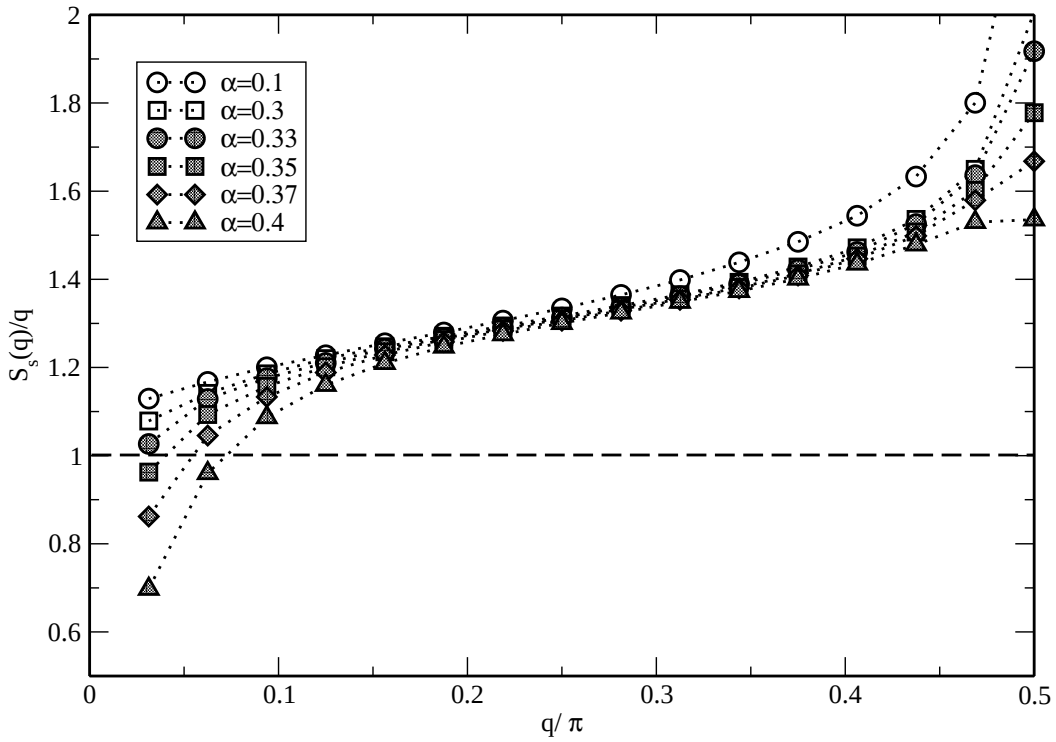

Figure 3.4 Spin Structure factor vs q for $\omega = 0.2$ for $U = 6$ and $V = 1$. $\alpha_c \approx 3.1$.

Fig:3.4 shows spin structure factor vs q for $\omega = 0.2$, $U = 6$ and $V = 1$ for $L = 32$. The curves for $\alpha > \alpha_c$ (filled symbols) dip below 1, indicating opening of a spin gap.

3.4 Comparison of α_c to 1/2-filled

We use the dimerized model to study the spin gap because dimerization is necessary to observe a SP transition at quarter filling as described before in Chapter 1. We have chosen the amount of dimerization as $t_1 = 1.2$ and $t_2 = 0.8$, based on typical bond lengths for quasi-1D superconductors.

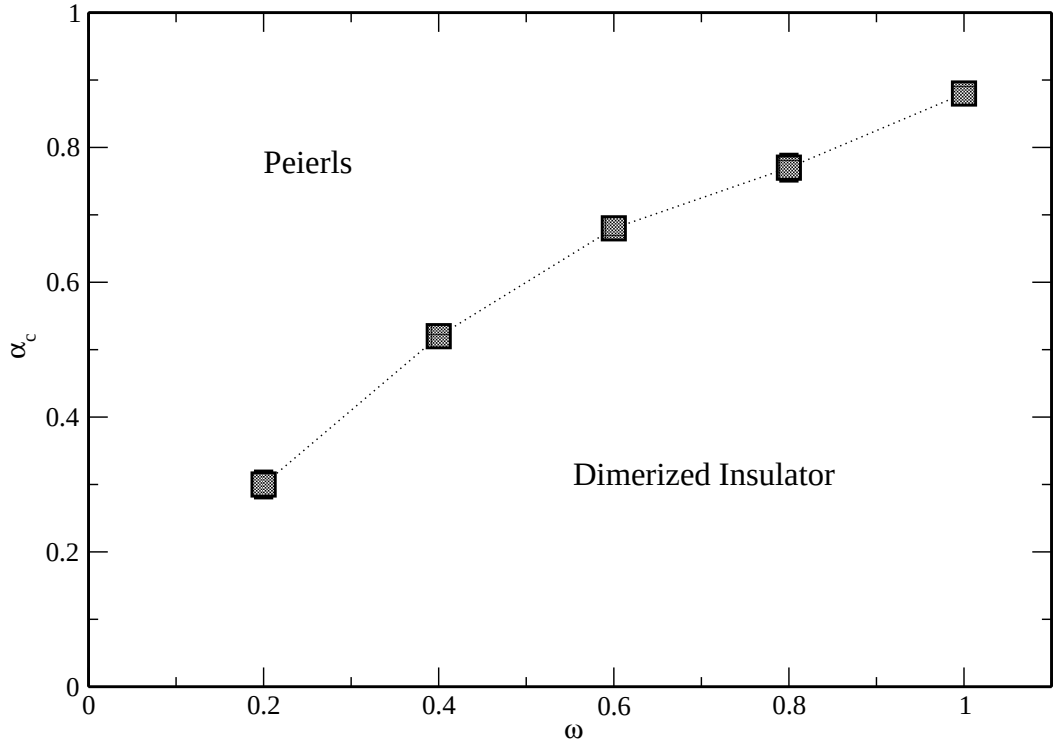

Figure 3.5 Determination of α_c for various ω for $U = 6$ and $V = 1$.

Previous study indicate that the critical coupling depends on the parameters of the Hamiltonian, specifically the bare phonon frequency ω.

We have determined the value of α_c at quarter filling as a function of finite bare phonon frequency ω keeping $U = 6$ and $V = 1$. Fig:3.5 shows a linear dependence of α_c over several ω. In comparison to half filling in [25] the α_c is higher for quarter filled state.

Using the above criteria we distinguishing the DI and Peierls phases. As compared to [25] we see that the DI state becomes more dominant as ω increases.

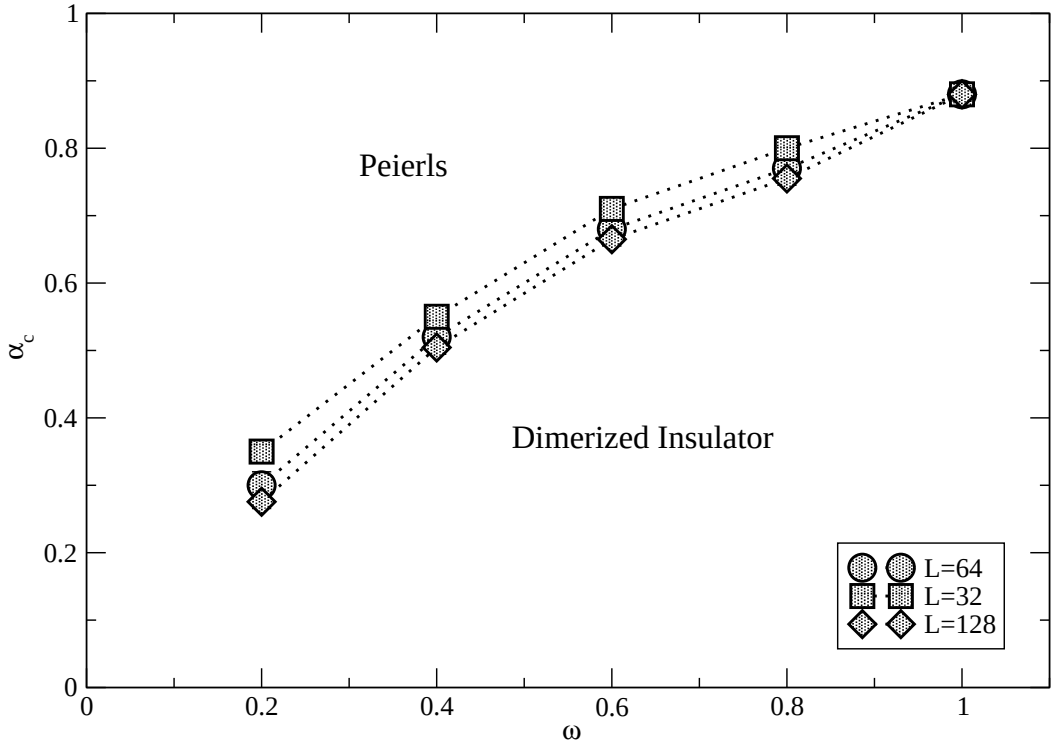

Figure 3.6 Finite size effects for Phase boundary between Peierls and Dimerized Insulator phase.

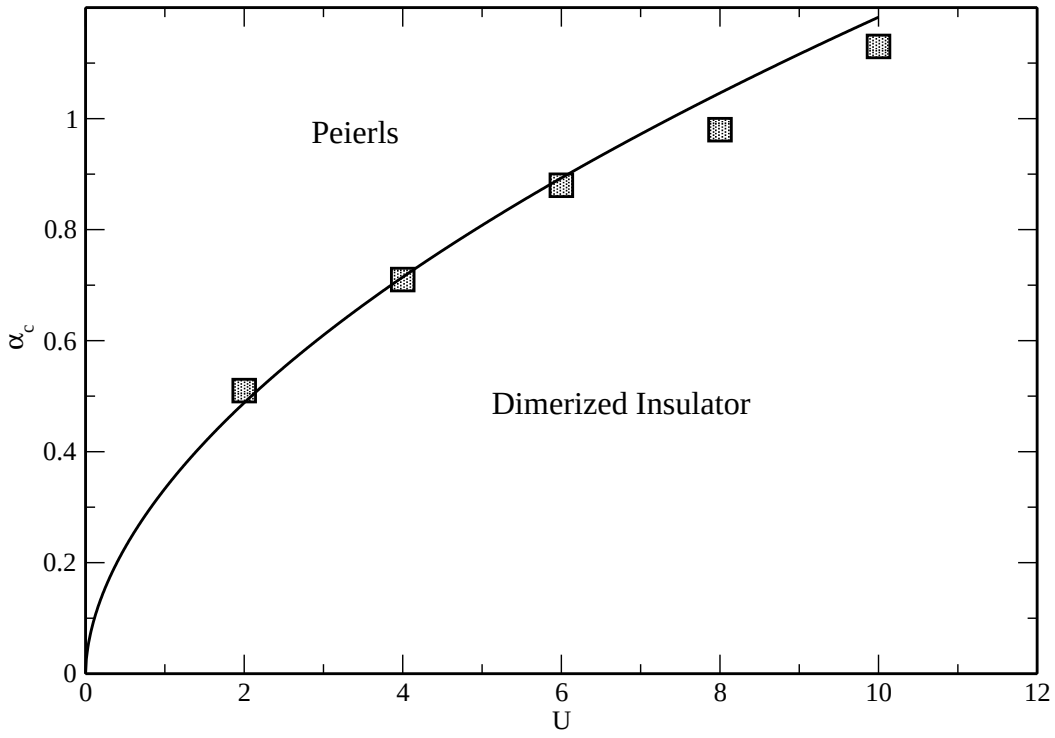

Figure 3.7 U vs α_c for $V = 1$ and $\omega = 1.0$.

In Fig:3.7 we find the value of α_c for $V = 1, \omega = 1.0$ for different U. It is apparent that LL phase is dominant for higher values of U. We also establish that $\alpha_c \sim U^{\gamma}$ where $\gamma = 0.55$ which is higher compared to $\gamma = 0.3$ for half filling [25].

In the next five plots we compare the order parameters for Phonons and no phonon case for system size L=32 with different $T = t/\beta$.

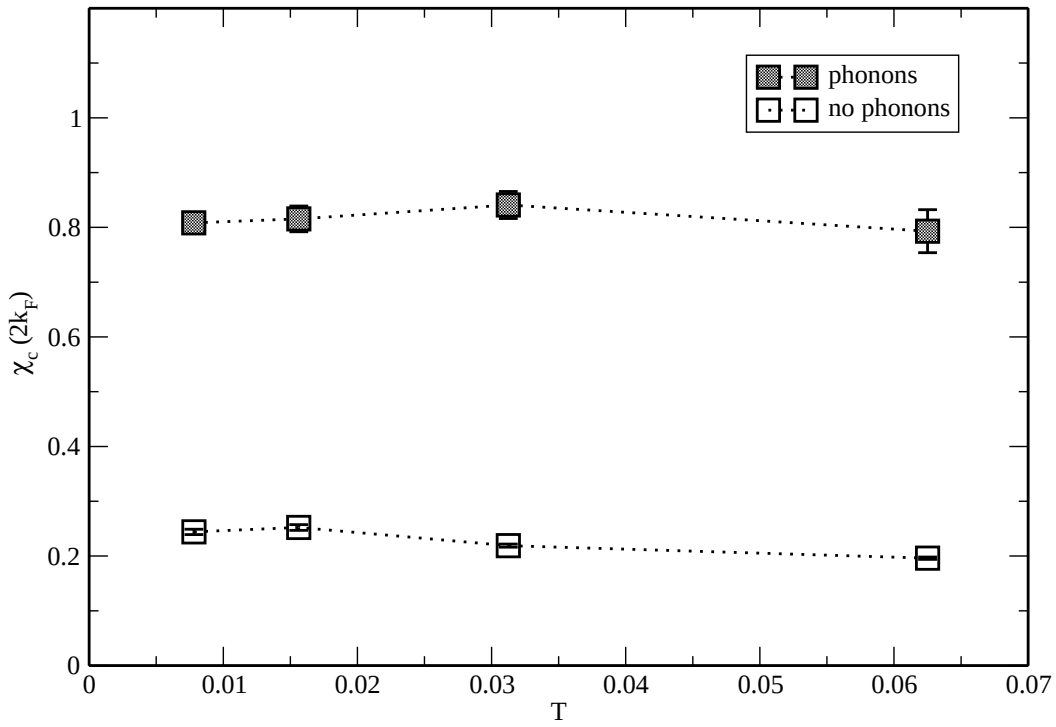

Figure 3.8 Comparison of Charge Susceptibility (χ_c) Vs Temperature (T) $2k_F$ peaks for Phonons and No Phonons at $U = 6$ and $V = 1$.

Fig:3.8 shows a smooth behaviour of $\chi_c(2k_F)$ peaks for various temperature for both phonon and no phonon cases. The $\chi_c(2k_F)$ values for the phonon case have large peak compared to no phonon case at particular temperature.

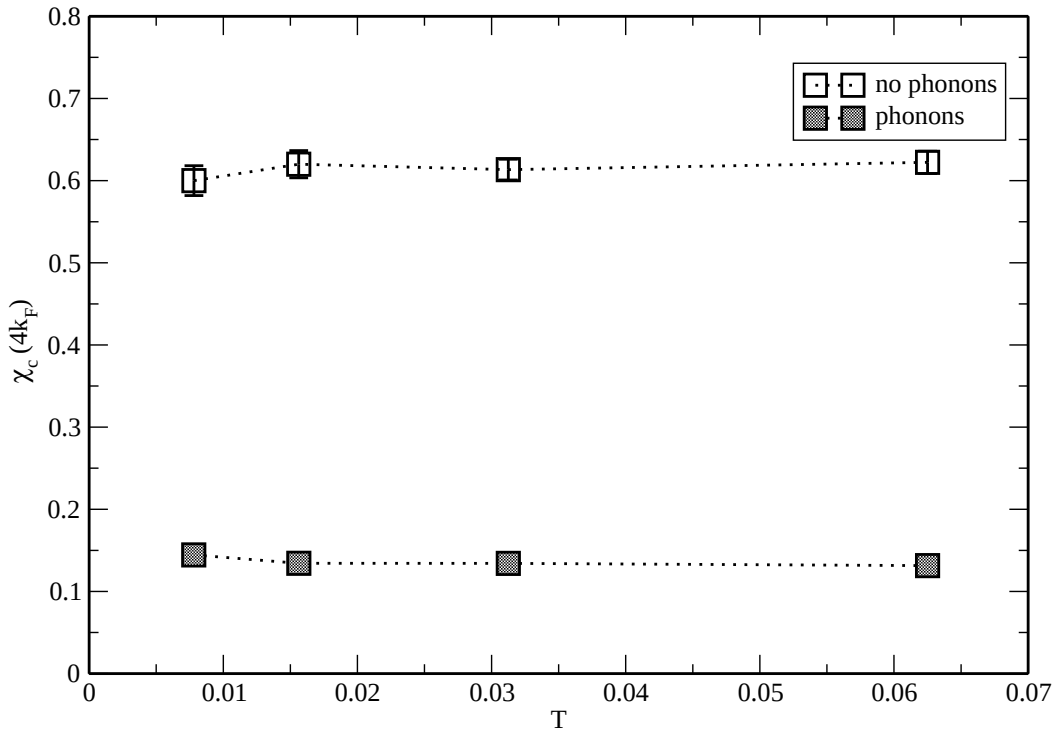

Figure 3.9 Comparison of Charge Susceptibility (χ_c) Vs Temperature (T) $4k_F$ peaks for Phonons and No Phonons at $U = 6, V = 1$ and L=32.

Fig:3.9 shows a smooth behaviour of $\chi_c(4k_F)$ peaks for various temperature for both phonon and no phonon cases. The $\chi_c(4k_F)$ peak is weaker for the phonon case compared to no phonon case at particular temperature.

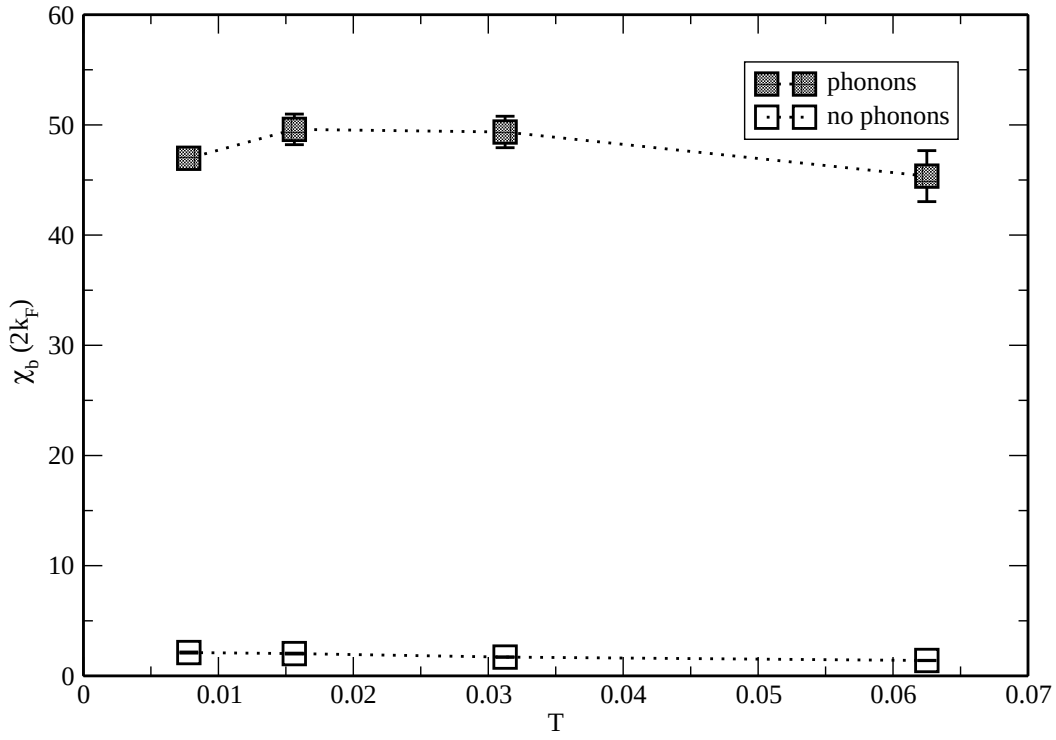

Figure 3.10 Comparison of Bond Order Susceptibility (χ_b) Vs Temperature (T) $2k_F$ peaks for Phonons ($\omega = 1.0$ and $\alpha = 0.9$) and No Phonons at $U = 6, V = 1$ and L=32.

Fig:3.10 shows a smooth behaviour of $\chi_b(2k_F)$ peaks for various temperature for both phonon and no phonon cases. The $\chi_b(2k_F)$ peak is higher for the phonon case compared to no phonon case at particular temperature. The $\chi_b(4k_F)$ peaks for the phonon case are not compared, as the system is explicitly dimerized.

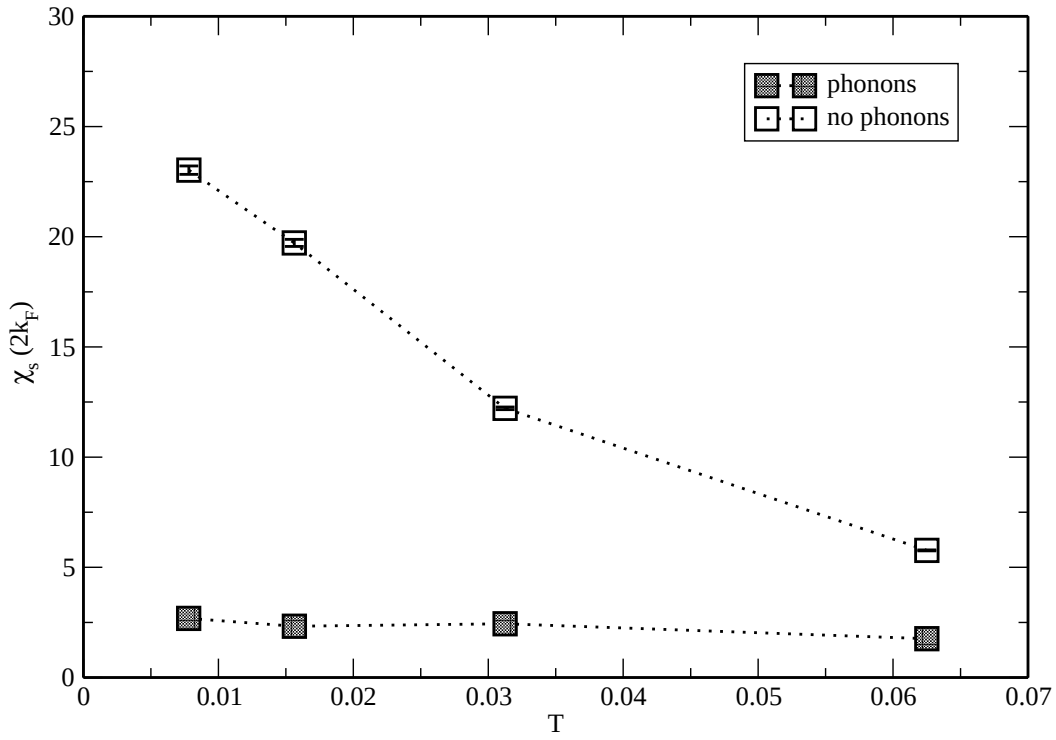

Figure 3.11 Comparison of Spin Susceptibility (χ_s) Vs Temperature (T) $2k_F$ peaks for Phonons ($\omega = 1.0$ and $\alpha = 0.9$) and No Phonons at $U = 6, V = 1$ and L=32.

Fig:3.11 shows the behaviour of $\chi_s(2k_F)$ peaks for various temperature for both phonon and no phonon cases. The $\chi_s(2k_F)$ peak for phonon case decreases as T is increased showing that the $\chi_s(2k_F)$ weakens with increase with temperature. Initially the phonon $\chi_s(2k_F)$ is higher that the no phonon case but as temperature is increased the phonon $\chi_s(2k_F)$ approaches the no phonon $\chi_s(2k_F)$ peak. In the phonon case the spin susceptibility weakens indicating a spin gap state.

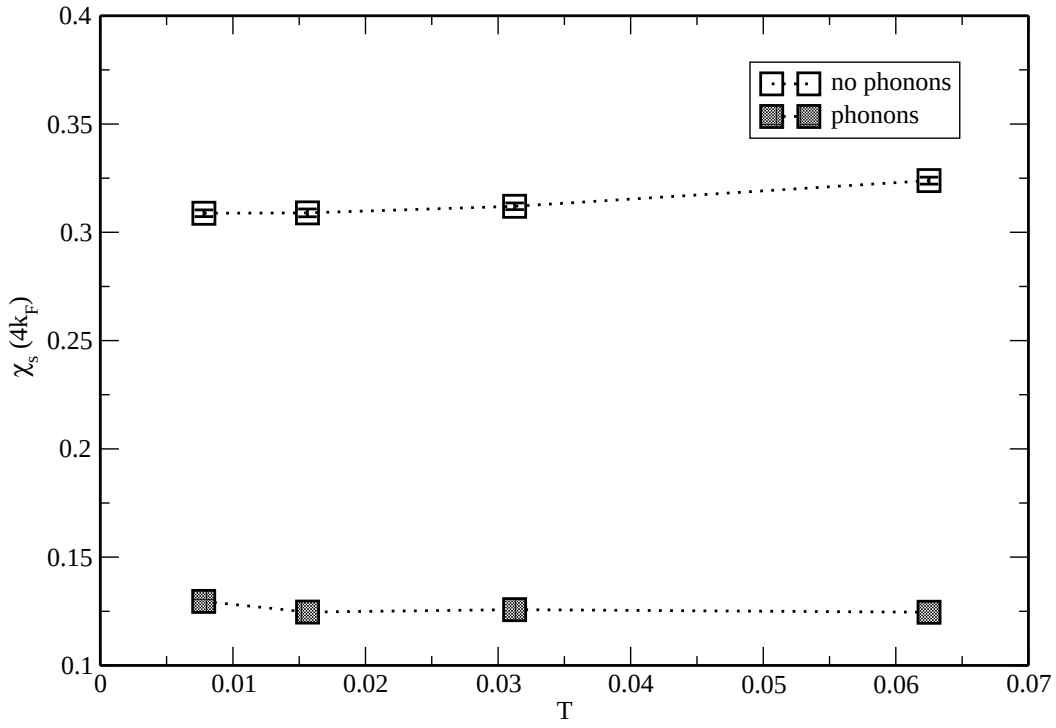

Figure 3.12 Comparison of Spin Susceptibility (χ_s) Vs Temperature $4k_F$ peaks for Phonons ($\omega = 1.0$ and $\alpha = 0.9$) and No Phonons at $U = 6, V = 1$ and L=32.

Fig:3.12 shows the behaviour of $\chi_s(4k_F)$ peaks for various temperature for both phonon and no phonon cases. The $\chi_s(4k_F)$ peak for phonon case shows a little fluctuations as T is increased but $\chi_s(4k_F)$ is weaker in case of phonons than no phonon case.

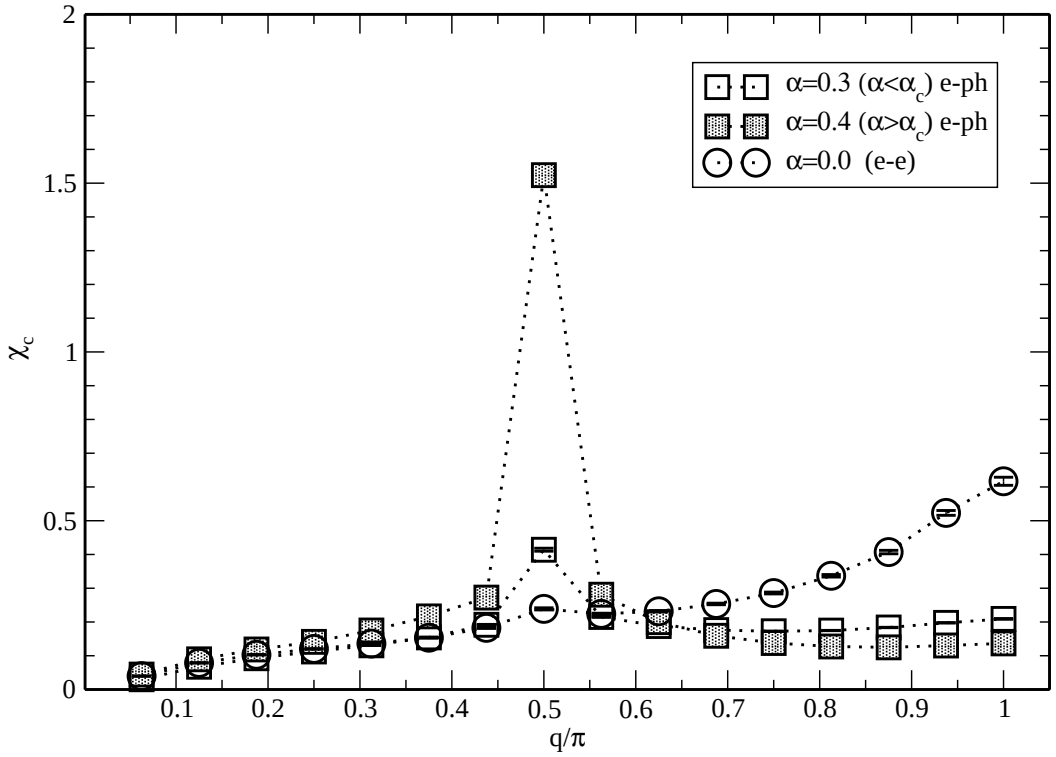

Figure 3.13 Comparison of $2k_F$ and $4k_F$ peaks for Charge susceptibility.

Fig:3.13 shows comparison of $2k_F$ and $4k_F$ peaks for Charge susceptibility of EHM and PEH for $\omega \sim 0$. Shown are the data three data sets(1) pure EHM (open squares) i.e. $\alpha = 0$ and $\omega = 0$, (2)PEH with $\omega = 0.2$ and $\alpha_c > \alpha$, and (3) PEH with same omega but $\alpha_c < \alpha$. It clearly shows that value for $2k_F$ peak increases as we go to higer value α in

PEH while the $4k_F$ peak shows a decrease. Also as $q \to 0, \chi_C \to 0$ indicating opening of a spin gap.

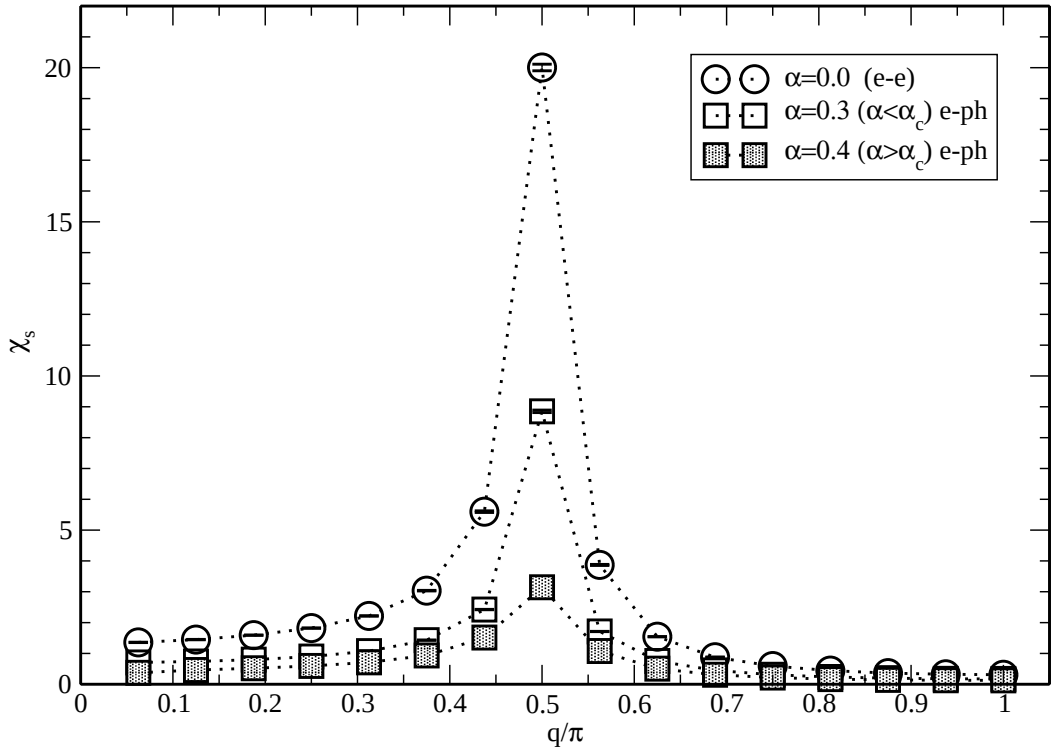

Figure 3.14 Comparison of $2k_F$ and $4k_F$ peaks for Spin susceptibility.

The data sets are for the same parameters but with respect to spin susceptibility. The above plot clearly indicates that $2k_F$ peak weakens as we go to higher value of α. Also a thing to note is that as $q \to 0, \chi_s \to$ constant value again conforming presence of spin gap.

3.5 Table of μ for various coupling α

For half-filling the value of chemical potential μ is zero. But at quarter-filling the value of μ varies with respect to other parameters. Following table gives some idea about how μ changes with change in on-site interactions U and α.

Table 3.1 Change in μ as a function of U and α.

U	V	μ	α	ω	β	ρ	$t1$	$t2$
2	1	4.02	0.51	1.0	64.0	0.5	1.2	0.8
4	1	4.60	0.60	1.0	64.0	0.5	1.2	0.8
6	1	5.40	0.87	1.0	64.0	0.5	1.2	0.8
8	1	5.85	0.80	1.0	64.0	0.5	1.2	0.8
10	1	6.60	1.00	1.0	64.0	0.5	1.2	0.8

CHAPTER IV

CONCLUSIONS

In conclusion we, one by one list all the new results we got for the Peierls Extended Hubbard model at 1/4 filling.

The phase boundary for ..1010.. CDW and the LL phase is shifted in upwards PEH in comparison to EHM indicating weakening of ..1010.. CDW phase due to the presence of bond phonons. Also for finite $U >> 0$, $V_c(U) \approx 2.5$ and finite $V >> 0$, $U_c(V) \approx 4$. The $U_c(V)$ boundary agrees with the EHM boundary for LL and ..1010.. CDW. The phase boundary dependence on size of the lattice is negligible.

We report the Energy autocorrelation time for the SSE method. At quarter filling the autocorrelation time τ grows exponentially for coupling α close to and greater than critical coupling α_c. Clearly some improvement must be made to access system with $\alpha > \alpha_c$. The autocorrelation time for EHM is comparable to that of PEH at $\alpha \sim 0$.

There is a linear dependence of coupling α_c for various bare phonon frequency ω . Finite-size scaling for different system sizes indicate a very little deviation of the phase boundary. Also the value of critical coupling for quarter filling is higher as compared to the half filled case.

Study of α_c value for $V = 1$ and different U indicates that $\alpha_c \sim U^{0.55}$ at quarter filling with $\omega = 1.0$ and dimerization with bond lengths $t_1 = 1.2$ and $t_2 = 0.8$.

4.1 Open Issues

Following are some open issues which we will be dealing with next in our research:

- Determination of magnitude of spin gap for finite as well as infinte lattice for quarter filling at a value of coupling α much higher that the critical value.
- Can spin gap happen in 1010 state for large value of V?
- Improvement of SSE method with phonons to lower autocorrelation time τ.
- Determination of magnitude of spin gap vs α for $\alpha > \alpha_c$.
- Similar study for ..1010.. charge ordered state and its comparison with present results.

REFERENCES

[1] N. W. Ashcroft and N. D. Mermin, *Solid State Physics*, Brooks-Cole, 1976.

[2] J. Cannon, R. Scallettar, , and E. Fradkin, "Ground-state phase diagram of the one-dimensional extended Hubbard model," *Phys. Rev B*, vol. 44, no. 12, Sept. 1991, pp. 5995–6001.

[3] R. T. Clay, S. Mazumdar, , and D. K. Campbell, "Pattern of charge ordering in quasi-one-dimensional organic charge-transfer solids," *arXiv: cond-mat*, vol. 1, no. 0112278, Dec. 2001, pp. 1–19.

[4] R. T. Clay, S. Mazumdar, , and D. K. Campbell, "Pattern of charge ordering in quasi-one-dimensional organic charge-transfer solids," *Phys. Rev B*, vol. 67, no. 115121, Mar. 2003, pp. 1–9.

[5] R. T. Clay, A. W. Sandvik, , and D. K. Campbell, "Possible exotic phases in the one-dimensional extended Hubbard model," *Phys. Rev. B*, vol. 59, no. 7, Feb. 1999, pp. 4665–4679.

[6] E. Dagotto, "Correlated electrons in high-temperature superconductors," *Reviews of Modern Physics*, vol. 66, no. 3, July 1994, pp. 763–840.

[7] L. M. del Bosch and L. M. Falicov, "Extended one-dimensional Hubbard Model: A small-cluster approach," *Phys. Rev B*, vol. 37, no. 11, Aug. 1988, pp. 6073–6078.

[8] K. B. Efetov and A. I. Larkin, ," *Sov. Phys. JETP*, vol. 42, no. 390, 1976.

[9] V. J. Emery, "Theory of the quasi-one-dimensional electron gas with stron "on-site" interactions," *Phys. Rev B*, vol. 14, no. 7, Oct. 1976, pp. 2989–2994.

[10] V. J. Emery, *Highly Conducting One-Dimensional Solids*, Plenum, New York, 1979.

[11] B. Fourcade and G. Spronken, "Real-space scaling methods applied to the one-dimensional extended Hubbard model. I. The real-space renormalization-group method.," *Phys. Rev. B*, vol. 29, no. 9, July 1984, pp. 5089–5095.

[12] B. Fourcade and G. Spronken, "Real-space scaling methods applied to the one-dimensional extended Hubbard model.II. The finite-cell scaling method.," *Phys. Rev. B*, vol. 29, no. 9, May 1984, pp. 5096–5102.

[13] M. Fowler, "Theory of the quasi-one-dimensional electron gas with strong "on site" interaction.," *Phys. Rev B*, vol. 17, no. 7, Sept. 1978, pp. 2989–2993.

[14] F. D. M. Haldane, "General Relation of Correlation Exponents and Spectral Properties of One-Dimensional Fermi Systems: Application to the Anisotropic S=1/2 Heisenberg Chain," *Phys. Rev. Lett.*, vol. 45, no. 16, Oct. 1980, pp. 1358–1362.

[15] F. D. M. Haldane, "'Luttinger liquid theory' of one-dimensional quantum fluids. I. Properties of the Luttinger model and their extension to the general 1D interacting spinless Fermi gas," *J. Phys. C*, vol. 14, no. 2585–2609, 1981.

[16] J. E. Hirsch, "Charge-Density-Wave to Spin-Density Wave Transition in the Extended Hubbard Model," *Phys. Rev. Lett.*, vol. 53, no. 24, Dec. 1984, pp. 2327–2330.

[17] J. E. Hirsch and D. J. Scalapino, "$2p_F$ and $4p_F$ instabilities in a one-quarter-filled band Hubbard model," *Phys. Rev B*, vol. 27, no. 12, June 1983, pp. 7169–7185.

[18] J. E. Hirsch and D. J. Scalapino, "$2p_F$ and $4p_F$ instabilities in the one-dimensional Hubbard model," *Phys. Rev B*, vol. 29, no. 10, May 1984, pp. 5554–5561.

[19] H. Q. Lin, D. K. Campbell, , and R. T. Clay, "Broken Symmetries in the One-Dimensional Extended Hubbard Model," *Chinese Journal of Physics*, vol. 38, no. 1, 2000.

[20] H. Q. Lin, E. R. Gagliano, D. K. Campbell, E. H. Fradkin, and J. E. Gubernatis, "The Phase Diagram of the Extended Hubbard Model in One Dimension for Arbitrary Band Filling," April 1995, p. 42.

[21] H. Q. Lin and J. E. Hirsch, "Condensation transition in the one-dimensional extended Hubbard model," *Phys. Rev B*, vol. 33, no. 12, June 1986, pp. 8155–8163.

[22] J. M. Luttinger, "An Exactly Soluble Model of a Many-Fermion System," *J. Math. Phys.*, vol. 4, no. 1154, 1963.

[23] S. Mazumdar, H. Q. Lin, and D. K. Campbell, *Organic Superconductivity*, Plenum, 1990.

[24] D. Poilblanc, T. Siman, J. Bellisard, F. Mila, , and G. Montambaux, "Poisson versus GOE statistics in integrable and non-integrable quantum Hamiltonians," *Europhys. Lett.*, vol. 22, 1993, pp. 537–542.

[25] P. Sengupta, A. W. Sandvik, , and D. K. Campbell, "Peierls transition in the presence of finite-frequency phonons in the one-dimensional extended Peierls-Hubbard model at half-filling," *Phys. Rev. B*, vol. 67, no. 245103, June 2003, pp. 1–6.

[26] J. Solyom, "The Fermi gas model of one-dimensional conductors," *Adv. in Physics*, vol. 28, no. 2, 1979, pp. 201–303.

[27] O. F. Syljuasen and A. W. Sandvik, "Quantum Monte Carlo with directed loops," *Phys. Rev. E*, vol. 66, no. 046701, Oct. 2002, pp. 1–28.

[28] H. Tasaki, "The Hubbard Model-Introduction and Selected Rigorous Results," *arXiv:cond-mat*, vol. 4, no. 9512169, Dec. 1997, pp. 1–33.

[29] S. Tomonaga, ," *Prog. Theor. Phys.*, vol. 5, no. 544, 1950.

APPENDIX

LANCZOS CODE

As mentioned in Chapter 2 we use Lanczos method to verify the results from the Stochastic Series Expansion. Following is a C code for Lanczos Method. This code gives the energy eigen value, density and wavefunction for system size till L=16 for Extended Hubbard Model. This code is developed by me and I have used “SPRNG” random number generator.

```
#include <stdio.h>
#include <math.h>
#include "nrutil.h"
#include "nrutil.c"
#include "voidtqli.c"
#define NSITES NS
#define NUP NU
#define NDN ND
#define MAXSTEPS 200
#define DENS
#define WAVEFUN
FILE *fi, *fopen();
int fclose();
FILE *fo;
char FILENAME[80];
char tmp[80];
int NS,NU,ND;
float u,v;
int ib,*HOP_MASK_1,*HOP_MASK_2,*HOP_MASK,*SITE_MASK,*charge;
double *b,*q,*V,*U,*WF,*density;
int *JUP,*JDN;
int IUPMIN,IUPMAX,IDNMIN,IDNMAX,NSUP,NSTATES,IUP,IDN,jend;
int count_ne(int IUP);
int count_dn(int IDN);
double randomb();
int HOPMASK1();
int HOPMASK2();
int HOPMASK();
int SITEMASK();
void call(double *qin,double *qout);
void dens();
main(int narg, char **arg)
{
  unsigned int j;
  int file_arg;
  int k,i,R,PMAX,PMIN,PMIN1,PMAX1,d1,index;
  long int kuu,kdd;
  double norm,t,**z,temp,templast,*alpha,*alphatemp,*beta,*betatemp,*y,eps;
  static char *rst = "-r";
  file_arg=1;
  if (narg > 1) {
    for (i = 1; i < narg; i++) {
      if (!strcmp(rst, arg[i])) {

      } else {
        file_arg = i;
        strcpy(FILENAME, arg[file_arg]);
      }
    }
```

```
}
fi=fopen(FILENAME,"r");
fscanf(fi,"%d",&NS);
fscanf(fi,"%d",&NU);
fscanf(fi,"%d",&ND);
fscanf(fi,"%f",&u);
fscanf(fi,"%f",&v);
fclose(fi);

jend=pow(2,NSITES-1);

PMAX=0;
j=jend;
for(i=0;i<NUP;i++)
  {
    PMAX=PMAX+j;
    j=j>>1;
  }

PMIN=0;
j=1;
for(i=0;i<NUP;i++)
  {
    PMIN=PMIN+j;
    j=j<<1;
  }

PMAX1=0;
j=jend;
for(i=0;i<NDN;i++)
  {
    PMAX1=PMAX1+j;
    j=j>>1;
  }
PMIN1=0;

j=1;
for(i=0;i<NDN;i++)
  {
    PMIN1=PMIN1+j;
    j=j<<1;
  }

sprintf(tmp,"%s.dat", FILENAME);
fo=fopen(tmp,"w");
fprintf(fo,"------------------Lanczos algorithm for------------------\n ");
fprintf(fo,"Number of Sites=%d\n",NS);
fprintf(fo,"Number of Up electrons=%d\n",NU);
fprintf(fo,"Number of Down electrons=%d\n",ND);
fprintf(fo,"Onsite interaction energy=%g\n",u);
fprintf(fo,"Intersite interaction energy=%g\n",v);
fprintf(fo,"------------------------------------------------------------\n ");


JUP=ivector(PMIN,PMAX);
JDN=ivector(PMIN1,PMAX1);
HOP_MASK_1=ivector(0,NSITES-1);
HOP_MASK_2=ivector(0,NSITES-1);
HOP_MASK=ivector(0,NSITES-1);
SITE_MASK=ivector(0,NSITES-1);
charge=ivector(0,NSITES-1);
density=dvector(0,NSITES-1);
V=dvector(0,NSITES-1);
```

```
U=dvector(0,NSITES-1);
z=dmatrix(1,MAXSTEPS,1,MAXSTEPS);
alpha=dvector(0,MAXSTEPS-1);
alphatemp=dvector(0,MAXSTEPS-1);
beta=dvector(0,MAXSTEPS-1);
betatemp=dvector(0,MAXSTEPS-1);
y=dvector(0,MAXSTEPS-1);

IUPMIN=0;
j=1;
for(k=0;k<NUP;k++)
  {
    IUPMIN=IUPMIN|j;
    j=j<<1;
  }

IUPMAX=0;
j=jend;
for(k=NSITES;k>NSITES-NUP;k--)
  {
    IUPMAX=IUPMAX|j;
    j=j>>1;
  }

IDNMIN=0;
j=1;
for(k=0;k<NDN;k++)
  {
    IDNMIN=IDNMIN|j;
    j=j<<1;
  }

j=jend;
IDNMAX=0;
for(k=NSITES;k>NSITES-NDN;k--)
  {
    IDNMAX=IDNMAX|j;
    j=j>>1;
  }
kuu=1;

for(IUP=IUPMIN;IUP<=IUPMAX;IUP++)
  {
    if(count_ne(IUP)!=NUP)
      {
        JUP[IUP]=0;
        continue;
      }
    else
      {
        JUP[IUP]=kuu;
        kuu++;
      }
    NSUP=kuu-1;
  }

kdd=1;
d1=1;
for(IDN=IDNMIN;IDN<=IDNMAX;IDN++)
  {
    if(count_dn(IDN)!=NDN)
      {
        JDN[IDN]=0;
```

```
        continue;
      }
    else
      {
        JDN[IDN]=kdd;
        kdd+=NSUP;
        d1++;
      }
  }

NSTATES=(kuu-1)*(d1-1);

b=dvector(1,NSTATES);
q=dvector(1,NSTATES);
WF=dvector(1,NSTATES);
randomb();

for(i=1;i<=NSTATES;i++)
  {
    q[i]=0.0;
  }

norm=0.0;
for(i=1;i<=NSTATES;i++)
  {
    norm+=b[i]*b[i];
  }
norm=sqrt(norm);

for(i=1;i<=NSTATES;i++)
  {
    b[i]/=norm;
  }
HOPMASK1();
HOPMASK2();
HOPMASK();
SITEMASK();
/*First Run of Lanczos subroutine to get lowest energy eigen value*/
R=0;
beta[1]=0.0;

while(R<MAXSTEPS)
  {
    if(R!=0)
      {
        {
          for(i=1;i<=NSTATES;i++)
            {
              t=b[i];
              b[i]=q[i]/beta[R];
              q[i]=-beta[R]*t;
            }
        }
      }

    call(b,q);
/*****************Defining unit matrix*************************/
    if(R>1)
      {
        for(i=1;i<=R;i++)
          {
            for(k=1;k<=R;k++)
              {
```

```
                if(i!=k){
                  z[i][k]=0.0;
                }
                else{
                  z[i][k]=1.;
                }
              }
            }
          }
        /*************************************************************************/
        R+=1;
        alpha[R]=0.0;

        for(i=1;i<=NSTATES;i++)
          {
            alpha[R]+=b[i]*q[i];
          }

        for(i=1;i<=NSTATES;i++)
          {
            q[i]=q[i]-alpha[R]*b[i];
          }

        norm=0.0;
        for(i=1;i<=NSTATES;i++)
          {
            norm+=q[i]*q[i];
          }
        norm=sqrt(norm);
        beta[R]=norm;

        for(i=1;i<=R;i++){
          betatemp[i]=beta[i];
          alphatemp[i]=alpha[i];
        }

        if (R>1)
          {
            tqli(alphatemp,betatemp-1,R,z);
/*****Choosing the minimum energy eigen value and
       finding the index associated with it and
       assigning to y[i] array*********/
            temp=alphatemp[1];
            index=1;
            for (i=2;i<=R;i++)
              {
                if(alphatemp[i]<temp){
                  temp=alphatemp[i];
                  index=i;}
              }
            eps=temp/NS;
            fprintf(fo,"Lowest Energy=%f and Energy/NSITES=%f\n",temp,eps);

            if(templast-temp<pow(10,-6)){
              break;
            }
            else{
              templast=temp;
            }
          }
      }

     for(i=1;i<=R;i++){
```

```
   y[i]=z[i][index];
 }
 fprintf(fo,"-------------------------------------------------\n");
 fclose(fo);
 /*Second Run of lanczos subroutine
   except tqli to calculate wavefunction*/
 randomb();
 norm=0;
 for(i=1;i<=NSTATES;i++)
   {
     norm+=b[i]*b[i];
   }
norm=sqrt(norm);

for(i=1;i<=NSTATES;i++)
  {
    b[i]/=norm;
    q[i]=0.0;
    WF[i]=0.0;
  }
for(i=1;i<=NSTATES;i++)
  {
    WF[i]=0.0;
  }

R=0;
beta[1]=0.0;
while(R<=MAXSTEPS)
  {
    if(R!=0)
      {
        for(i=1;i<=NSTATES;i++)
          {
            t=b[i];
            b[i]=q[i]/beta[R];
            q[i]=-beta[R]*t;

          }
      }

    call(b,q);

    R+=1;


    alpha[R]=0.0;

    for(i=1;i<=NSTATES;i++)
      {
        alpha[R]+=b[i]*q[i];

      }
    for(i=1;i<=NSTATES;i++)
      {
        q[i]=q[i]-alpha[R]*b[i];

      }

    norm=0;
    for(i=1;i<=NSTATES;i++)
      {

        norm+=q[i]*q[i];
```

```
      }

     norm=sqrt(norm);
     beta[R]=norm;

     for(i=1;i<=NSTATES;i++)
       {
         WF[i]+=y[R]*b[i];
       }

   }
 /*********Normalizing the Wavefunction**********/
#ifdef WAVEFUN
 sprintf(tmp,"%s-wavfn.dat", FILENAME);
 fo=fopen(tmp,"w");
#endif
 norm=0;
 for(i=1;i<=NSTATES;i++)
   {
     norm+=WF[i]*WF[i];
   }
 norm=sqrt(norm);
 for(i=1;i<=NSTATES;i++)
   {
     WF[i]=WF[i]/norm;

#ifdef WAVEFUN
     fprintf(fo,"Wavefunction%d=%g\n",i,WF[i]);
#endif
   }
#ifdef WAVEFUN
 fclose(fo);
#endif
 /*********************************************/
 dens();

}

int count_ne(int IUP)
{
  int count,i;
  unsigned int j;
  j=1;
  count=0;
  for(i=1;i<=NSITES;i++)
    {
      if(IUP&j)
        {
          count++;

        }
      j<<=1;
    }

  return count;

}

int count_dn(int IDN)
{
  int count,i;
  unsigned int j;
```

```
  j=1;
  count=0;
  for(i=1;i<=NSITES;i++)
    {
      if(IDN&j)
        {

          count++;

        }
      j<<=1;
    }

  return count;
}
/**********Find density of electrons***************/
void dens()
{
  int J;
  int chg;
#ifdef DENS
  sprintf(tmp,"%s-dens.dat", FILENAME);
  fo=fopen(tmp,"w");
#endif
  for(IDN=IDNMIN;IDN<=IDNMAX;IDN++){
    if(!JDN[IDN]) continue;
    for(IUP=IUPMIN;IUP<=IUPMAX;IUP++){
      if(!JUP[IUP]) continue;
      J=JUP[IUP]+JDN[IDN]-1;
      for(ib=0;ib<NSITES;ib++){
        chg=0;
        if(HOP_MASK_1[ib] & IDN) chg++;
        if(HOP_MASK_1[ib] & IUP) chg++;
        charge[ib]=chg;
        density[ib]+=charge[ib]*pow(WF[J],2);
      }

    }
  }
  for(ib=0;ib<NSITES;ib++){
#ifdef DENS
    fprintf(fo,"density%d=%f\n",ib,density[ib]);
#endif
  }
#ifdef DENS
  fclose(fo);
#endif
}
/***************************************/

void call(double *qin,double *qout)
{
  int s,J,J2,n1,n2,ku,kd,lu,ld;
  double diag;

  for(IDN=IDNMIN;IDN<=IDNMAX;IDN++){
    if(!JDN[IDN]) continue;
    for(IUP=IUPMIN;IUP<=IUPMAX;IUP++){
      if(!JUP[IUP]) continue;
      J=JUP[IUP]+JDN[IDN]-1;
      diag=0.0;
      for(ib=0;ib<NSITES;ib++)
        {
```

```
          V[ib]=v;
          U[ib]=u;
        }
      for(ib=0;ib<NSITES;ib++){
        n1=0;
        n2=0;
        if(IUP & HOP_MASK_1[ib]) n1++;
        if(IDN & HOP_MASK_1[ib]) n1++;
        if(IUP & HOP_MASK_2[ib]) n2++;
        if(IDN & HOP_MASK_2[ib]) n2++;
        diag+=V[ib]*n1*n2;
        ku=(HOP_MASK[ib] & IUP);
        lu=ku^HOP_MASK[ib];
        kd=(HOP_MASK[ib] & IDN);
        ld=kd^HOP_MASK[ib];
        if(lu &&(lu!=HOP_MASK[ib]))
          {
            s=1;
            J2=JUP[IUP-ku+lu]+JDN[IDN]-1;
            qout[J2]+=-s*qin[J];
          }

        if(ld &&(ld!=HOP_MASK[ib]))
          {
            s=1;
            J2=JDN[IDN-kd+ld]+JUP[IUP]-1;
            qout[J2]+=-s*qin[J];
          }
      }
      for(ib=0;ib<NSITES;ib++){
        n1=0;
        n2=0;
        if(IUP & SITE_MASK[ib]) n1++;
        if(IDN & SITE_MASK[ib]) n2++;

        diag+=U[ib]*n1*n2;
      }
      qout[J]+=diag*qin[J];
    }
  }
}

/*********file declare.h*********/
#define NSITES NS
#define NUP NU
#define NDN ND
extern int NS,NU,ND;
extern int ib,*HOP_MASK_1,*HOP_MASK_2,*HOP_MASK,*SITE_MASK;
extern double *b,*q,*wf;
extern int *JUP,*JDN,NSTATES,jend;
extern int IUPMIN,IUPMAX,IDNMIN,IDNMAX,NSUP;
extern int IUP,IDN;
/*****************************/

/***********file hopmask************/
#include "declare.h"
int HOPMASK1()
{
  unsigned int j;

  j=1;
  for(ib=0;ib<NSITES;ib++)
    {
```

```
      HOP_MASK_1[ib]=j;

      j=j<<1;

    }
}
int HOPMASK2()

{
  unsigned int l;
  l=2;
  for(ib=0;ib<NSITES;ib++){
    HOP_MASK_2[ib]=l;

    l=l<<1;
    if(l>jend)

      {l=1;
      }
  }
}
int HOPMASK()
{
  unsigned int l,j;
  j=1;
  l=2;
  for(ib=0;ib<NSITES;ib++){
    HOP_MASK[ib]=j|l;

    j=j<<1;
    l=l<<1;
    if(l>jend)
      {l=1;
      }
  }

}
int SITEMASK()
{
  unsigned int j;
  j=1;

  for(ib=0;ib<NSITES;ib++)
    {
      SITE_MASK[ib] =j;


      j=j<<1;

    }
}
/*******file randomnum*******/
#define SIMPLE_SPRNG            /* simple interface  */
#include "sprng.h"              /* SPRNG header file*/
#include "declare.h"


double randomb()
{
  int i;
  int seed;
```

```
  seed = make_sprng_seed();

  init_sprng(10,SPRNG_DEFAULT);
  for(i=1;i<=NSTATES;i++)
    {
      b[i] = sprng();

    }
}
```